Model selection for spectral parameterization

Luc E. Wilson*, Jason da Silva Castanheira*, Benjamin Lévesque Kinder, Sylvain Baillet†
Montreal Neurological Institute, McGill University, Montreal QC, Canada

* These authors contributed equally: Luc E. Wilson, Jason da Silva Castanheira
† Corresponding author: sylvain.baillet@mcgill.ca.

Abstract: Neurophysiological brain activity comprises rhythmic (periodic) and arrhythmic (aperiodic) signal elements, which are increasingly studied in relation to behavioral traits and clinical symptoms. Current methods for spectral parameterization of neural recordings rely on user-dependent parameter selection, which challenges the replicability and robustness of findings. Here, we introduce a principled approach to model selection, relying on Bayesian information criterion, for static and time-resolved spectral parameterization of neurophysiological data. We present extensive tests of the approach with ground-truth and empirical magnetoencephalography recordings. Data-driven model selection enhances both the specificity and sensitivity of spectral and spectrogram decompositions, even in non-stationary contexts. Overall, the proposed spectral decomposition with data-driven model selection minimizes the reliance on user expertise and subjective choices, enabling more robust, reproducible, and interpretable research findings.

Lay summary: Brain activity is composed of rhythmic patterns that repeat over time and arrhythmic elements that are less structured. Recent advances in brain signal analysis have improved our ability to distinguish between these two types of components, enhancing our understanding of brain signals. However, current methods require users to adjust several parameters manually to obtain their results. The outcomes of the analyses therefore depend on each user's decisions and expertise. To improve the replicability of research findings, the authors propose a new, automated method to streamline the analysis of brain signal contents. They developed a new algorithm that defines the parameters of the analytical pipeline informed by the data. The effectiveness of this new method is demonstrated with both synthesized and real-world data. The new approach is made available to all researchers as a free, open-source app, observing best practices for neuroscience research.

Keywords: Neurophysiology, Spectral decomposition, Time-frequency analysis, Magnetoencephalography, Model selection, Rhythmic and arrhythmic brain signals, Parameter optimization, Reproducibility in research.

Introduction

Neural oscillations are rhythmic (periodic) signal components ubiquitously observed in electrophysiology across spatial and temporal scales (Buzsaki & Watson, 2012). In the power spectrum, periodic components can be modelled as Gaussian-shaped peaks emerging from an arhythmic (aperiodic) background (Wen & Liu, 2016; Donoghue et al., 2020; Wilson et al., 2022). Aperiodic activity is spectrally characterized by a reciprocal distribution of signal power that decays with frequency according to a power law ($1/f^{\alpha}$). In practice, the scalar exponent parameter α and broadband offset of the aperiodic model are inferred from estimates of the signal's power spectrum density (PSD) of the electrophysiological signal. Computational neuroscience models and growing empirical evidence suggest that α reflects the physiological balance between excitatory (E) and inhibitory (I) neural activity (Brake et al., 2024; Chini et al., 2022; Gao et al., 2017; Wiest et al., 2023), and the offset is related to aggregate neuronal population spiking (Miller et al., 2014; Voytek & Knight, 2015). These model parameters of the aperiodic spectral component decrease with age, accounting for the observation of a *flatter* power spectrum in aging (Cellier et al., 2021; Donoghue et al., 2020; Voytek et al., 2015). They also fluctuate during cognitive tasks (Donoghue et al., 2020; Gyurkovics et al., 2022; Preston et al., 2022; Waschke et al., 2021) and reflect behavioral traits (Ostlund et al., 2021; Wilson et al., 2022).

Recent algorithms and software such as the *specparam* (Donoghue et al., 2020) and Spectral Parameterization Resolved in Time (*SPRiNT;* Wilson et al., 2022) have streamlined the adoption of spectral parameterization in electrophysiological research. These tools require users to define a number of method parameters (hyperparameters), such as model complexity via the pre-specification of the maximum number of spectral peaks N_G to be adjusted from the empirical PSD (Gerster et al., 2022; Ostlund et al., 2022; Wilson et al., 2022). When hyperparameters are not set appropriately, the *specparam* algorithm either fits spurious, outlier spectral peaks or misses genuine spectral peaks (Donoghue et al., 2020). Similarly, time-resolved spectral parametrization tools rely on hyperparameters to minimize the detection of outlier spectral peaks (Brady & Bardouille, 2022; Cole et al., 2019; Kosciessa et al., 2020; Seymour et al., 2022; Stokes et al., 2023; Whitten et al., 2011; Wilson et al., 2022).

Setting model hyperparameters is a prevalent challenge across many fields of science and engineering. Good-practice approaches recommend prioritizing parsimonious models with a balance between simplicity (less hyperparameters) and the ability to fit the observed data (more flexibility; Vandekerckhove et al., 2015). Here, we propose such a model selection strategy for the parameterization of both the PSD and spectrogram of neurophysiological time series. The method proceeds with adjusting progressively more complex models to the empirical data spectrum or spectrogram, and determines the parameters of the simplest model that adequately accounts for the data on the basis of the Bayesian information criterion (BIC). This also enables the quantitation of evidence for periodic activity in spectral data via Bayes factor analysis. We demonstrate below the method's performance using extensive ground-truth simulated data and a large set of empirical resting-state magnetoencephalography (MEG) from N=606 participants.

Methods

Model Selection using Bayesian Information Criterion.

In the context of parsimonious modeling of power spectra and spectrograms, our goal is to optimize the trade-off between model fidelity and complexity. This principle emphasizes deriving the most accurate and representative model directly from empirical data while minimizing the inclusion of unnecessary assumptions or parameters (Myung, 2000). Among the methods for comparing models, Bayes factors are noteworthy as they balance model fit evaluation with the principle of simplicity (Jefferys & Berger, 1992). These factors can be effectively estimated using the Bayesian Information Criterion (BIC), which offers a pragmatic tradeoff between goodness-of-fit and complexity in terms of the number of model parameters (Schwarz, 1978; Vandekerckhove et al., 2015).

In the *specparam* approach, model fitting involves minimizing the least-squares error between model predictions and the empirical power spectrum. The *ms-specparam* method refines this objective by estimating the negative log-likelihood of a model:

$$-\ln p\,(\,y \mid x, w, \beta\,) = \frac{\beta}{2}\sum_{i=1}^{N}\{f(x_i, w) - y_i\}^2 - \frac{N}{2}\ln(\beta) + \frac{N}{2}\ln(2\pi)$$

where (x) and (y) are the frequency bins and empirical spectral power values, respectively; $(f(x_i, w))$ is the spectral power predicted by the model at frequency (x_i); (y_i) is the empirical spectral power value at frequency (x_i); (w) represents the model parameters, (N) the number of frequency bins. (β) is the precision, or inverse variance, of residuals.

$$\beta = 1/\sigma^2 \ ,$$

Under the assumption of zero-mean (unbiased) Gaussian noise in the empirical power spectrum, minimizing negative log-likelihood provides an equivalent solution to minimizing squared error (Mitchell, 1997). Finally, we express the *specparam* optimization's output in terms of the Bayesian information criterion (BIC):

$$\mathrm{BIC} = 2 \cdot \mathrm{NLL} + \log(N) \cdot k,$$

where NLL is the negative log-likelihood, (N) is the number of frequency bins, and (k) represents the total number of parameters, which includes the aperiodic parameters (exponent and offset) and three additional parameters for each peak (center frequency, amplitude, bandwidth). Note that $(k = 3P + 2)$, where (P) represents the number of peaks.

The *specparam* algorithm iteratively fits models of increasing complexity by adding peaks and minimizing the squared error. It performs a final optimization of both aperiodic and periodic parameters, and then converts the squared error into a negative log-likelihood, which is used to

calculate the BIC. The algorithm ultimately provides the parameters of the model with the lowest BIC, thus achieving a balance between fit quality and model simplicity.

We developed *ms-specparam* and *ms-SPRiNT* as plug-in libraries that interoperate with *Brainstorm* (Tadel et al., 2011) and are therefore open-source and accessible to everyone.

Algorithm Settings and Hyperparameters.

The spectral parameterization of neural power spectra (synthetic and empirical) was conducted in the frequency range of 1-40 Hz using three distinct approaches, each characterized by different hyperparameter settings:

1. Default Hyperparameters: This approach adhered to the default settings established by the Python implementation of *specparam* (Donoghue et al., 2020). The hyperparameters included a minimum peak height of 0.1 arbitrary units (a.u.), a maximum of 6 peaks, peak width limits set within the range of [1, 8] Hz, and a proximity threshold of 0.75 a.u.

2. **Conservative Hyperparameters:** This setting was driven by the *Brainstorm* implementation of *specparam* (Tadel et al., 2011). It involved more conservative hyperparameters, with a minimum peak height of 0.3 a.u., a reduced maximum number of peaks at 3, peak width limits broadened to [0.5, 12] Hz, and an increased proximity threshold of 2.0 a.u.

3. *ms-specparam*: This approach used the same hyperparameter settings as *default-specparam*, including a minimum peak height of 0.1 a.u., a maximum of 6 peaks, peak width limits between [1, 8] Hz, and a proximity threshold of 0.75 a.u. The most parsimonious spectral model is selected according to the procedure described in *Model Selection using Bayesian Information Criterion*.

These different spectral parameterization strategies were selected to provide a comprehensive comparison across various standard and conservative parameter settings.

Dynamic synthetic neural time series were similarly parameterized using *SPRiNT* in the 1-40 Hz frequency range, using 5x1 s windows (50% overlap), according to four distinct conditions. While each condition used default hyperparameters for *specparam*, they differed in their methodologies for removing spurious, outlier spectral peaks:

1. SPRiNT: No procedure for pruning spurious, outlier spectral peaks.

2. SPRiNT with post-processing: This condition identified putative spurious, outlier spectral peaks as those with fewer than a predetermined number of similar peaks (by center frequency) within neighboring time bins of the spectrogram. The process prunes identified spurious, outlier spectral peaks and re-optimizes spectral models in affected time bins. For more details, see Wilson et al. (2022). The hyperparameters used for post-processing consisted of pruning spectral peaks with fewer than four neighboring peaks within 1.5 Hz and six time bins (3 s).

3. ms-SPRiNT: This condition selected the most parsimonious spectral model in each time bin according to the procedure described in *Model Selection using Bayesian Information Criterion.*

4. ms-SPRiNT with post-processing: This process first selected the most parsimonious spectral model using *ms-SPRiNT* before pruning spurious, outlier spectral peaks through post-processing.

Synthetic Data.

We created 5,000 synthetic neural power spectra using a range of aperiodic parameters: exponents from 0.5 to 2 Hz^{-1}) and offsets from -8.1 to -1.5 arbitrary units (a.u.). Each power spectrum was augmented with zero to four peaks, with 1,000 instances for each peak quantity. The parameters for these peaks fell within specified ranges: center frequencies between 3 and 35 Hz, amplitudes from 0.1 to 1.5 a.u., and bandwidths (2 s.d.) from 2 to 6 Hz. We ensured a minimum separation of one bandwidth between adjacent peak frequencies. The frequency domain for simulation spanned from 0.5 to 100 Hz with increments of 0.5 Hz.

To mimic realistic noise conditions, we introduced Gaussian white noise at varying intensities: low (0.05 a.u.), medium (0.10 a.u.), and high (0.15 a.u.). We then applied *default-specparam* (minimum peak height of 0.1 a.u., up to six peaks, peak width range of 1 to 8 Hz, and proximity threshold of 0.75 a.u.) alongside *ms-specparam* with identical parameters.

We also used 10,000 synthetic neural-like time series to evaluate the model selection approach in the context of time-resolved spectral parameterization. These simulations, previously generated by Wilson et al. (2022) to evaluate *SPRiNT*'s performance, each consist of 60 seconds of unique, dynamic periodic and aperiodic activity. Aperiodic exponents were initialized between 0.8 and 2.2 Hz^{-1}, and aperiodic offsets between –8.1 and –1.5 a.u. Within the 12–36 second segment of the simulation (onset randomized), the aperiodic exponent and offset underwent a linear shift of magnitude in the ranges -0.5–0.5 Hz^{-1} and -1–1 a.u., respectively (sampled continuously and chosen randomly). The duration of the linear shift was randomly selected for each simulated time series between 6 and 24 seconds. Periodic components (0–4 peaks) were added to each trial with parameters randomly sampled within the ranges: center frequency: 3–35 Hz; amplitude: 0.6–1.6 a.u.; SD: 1–2 Hz. Onset (5–40 s) and duration (3–20 s) of periodic components (if any) were randomized across trials, with the constraint that they would not overlap in both time and frequency; they were allowed to overlap in one dimension. If a periodic component overlapped temporally with another, its center frequency was set at least 2.5 peak SDs from the other temporally overlapping periodic component(s). The magnitude of each periodic component was tapered by a Tukey kernel (cosine fraction = 0.4). Spectral noise levels were inherent to the methods for time-frequency decomposition (short-time Fourier transform, 5x1 s windows with 50% overlap) and were previously approximated to be high (approximately 0.2 a.u.; Wilson et al., 2022).

For accuracy assessment, a 'hit' was designated when an identified peak's center frequency was within one bandwidth (2 s.d.) of a true peak. In cases where multiple identified peaks met this criterion, the peak with the highest amplitude was selected as the 'hit.' Peaks detected by the algorithm that did not correspond to a true peak were classified as false positives.

We defined peak sensitivity as the ratio of 'hits' to the total number of simulated peaks, and the positive predictive value as the ratio of 'hits' to all detected peaks (including false positives). For

peaks identified as 'hits,' we calculated the parameter estimation error as the absolute deviation from the true values.

Bayes factor evidence for periodic brain activity.

Bayes factor (BF) provides a statistical measure for comparing two models, offering evidence about the presence of periodic activity within neural power spectra. The computation of the Bayes factor follows the formula proposed by Wagenmakers (2007):

$$\mathrm{BF}_{01} = e^{(\mathrm{BIC}_0 - \mathrm{BIC}_1)/2}$$

where (BIC_0) is the Bayesian Information Criterion (BIC) value for the aperiodic-only model and (BIC_1) is the BIC value of the lowest-BIC model.

In this context, (BIC_0) represents the BIC for the aperiodic-only model, which posits that the data can be explained without invoking rhythmic components. (BIC_1), on the other hand, corresponds to the model that includes both aperiodic and periodic elements and has the lowest BIC among all models considered.

The Bayes factor (BF_{01}) compares these models, translating the difference in their BIC values into the odds ratio against periodic activity. A smaller (BF_{01}) implies stronger evidence against the aperiodic-only model, thereby indicating the presence of significant periodic activity within the brain's neural power spectra. Conversely, larger (BF_{01})values suggest that the periodic components do not significantly improve the model beyond the aperiodic activity alone.

This approach allows for the quantitative assessment of oscillations in neural recordings, providing a more rigorous foundation for claims of rhythmic brain activity observed in electrophysiological data.

Empirical data.

The empirical dataset for our study was obtained from the Cambridge Centre for Aging Neuroscience repository (Cam-CAN; Shafto et al., 2014; Taylor et al., 2017). This comprehensive dataset includes 606 healthy individuals aged 18 to 90 years (mean age = 54.69; SD = 18.28), with a balanced gender representation (299 females). Each participant underwent a thorough assessment, beginning with a detailed home interview followed by a resting-state magnetoencephalography (MEG) session. The MEG recordings, lasting approximately 8 minutes each, were conducted using a 306-channel VectorView MEG system (MEGIN). These recordings were complemented with structural T1-weighted magnetic resonance imaging (MRI) to provide anatomical context for MEG source mapping. All data collection occurred at a single, consistent location to maintain uniformity in data acquisition.

This rich dataset forms the basis for our analyses, allowing for a comprehensive investigation into the spectral properties of neural signals across a wide age spectrum.

MEG Preprocessing and Source Mapping.

We preprocessed magnetoencephalography (MEG) data with Brainstorm (Tadel et al., 2011; March 2021 distribution), integrated with MATLAB (2020b; Natick, MA), adhering to established best-practice guidelines (Gross et al., 2015). The preprocessing methodology followed protocols detailed previously (da Silva Castanheira et al., 2021).

Line noise artifacts at 50 Hz and its first 10 harmonics were filtered using a notch filter bank. Additionally, an 88-Hz artifact present in the Cam-CAN dataset (Wiesman et al., 2022) was removed. To address slow-wave and DC-offset artifacts, a high-pass finite impulse response (FIR) filter with a cutoff frequency of 0.3 Hz was applied. Signal-Space Projections (SSPs) were implemented to attenuate cardiac artifacts and mitigate low-frequency (1–7 Hz) and high-frequency (40–400 Hz) noise components, typically originating from saccades and muscle activities.

Brain source models were anchored to the individual T1-weighted MRI data of each participant. Automatic segmentation and labeling of MRI volumes were achieved using FreeSurfer (Fischl, 2012). Co-registration with MEG data was facilitated using approximately 100 head points digitized for each participant. MEG biophysical head models were computed using *Brainstorm*'s overlapping-spheres model (default parameters).

Cortical source models were estimated using linearly constrained minimum-variance (LCMV) beamforming, following *Brainstorm*'s default parameters (2018 version for source estimation processes). MEG source orientations were constrained normal to the cortical surface, distributed across 15,000 locations. Neural power spectra were then calculated for each of the 148 cortical regions defined by the Destrieux atlas (Destrieux, 2010). These calculations were based on the first principal component of all signals within each region of interest (ROI). Neural spectral power was estimated using Welch's method, utilizing 2-second windows with a 50% overlap.

Statistical Analyses.

To evaluate the accuracy of spectral parameters generated by *ms-specparam*, we employed two-sample non-parametric permutation t-tests from the *RVAideMemoire* package in R. This statistical approach allowed us to test differences in spectral parameter estimates, specifically focusing on five key variables: aperiodic exponent, aperiodic offset, peak center-frequency, peak amplitude, and peak bandwidth.

To capture differences in residual variance and the number of peaks fitted between algorithms in our empirical data, we similarly relied on paired non-parametric permutation t-tests.

We implemented hierarchical linear regression models using the *lmer* function in R to test how algorithm choice impacts age's effect on both aperiodic exponent and offset. The models were formulated as:

$$y \sim \text{intercept} + (\text{Participant intercept}) + \beta_1 \times \text{chronological age} + \beta_2 \times \text{algorithm} + \beta_3 \times \text{chronological age} \times \text{algorithm}$$

where (y) represents the dependent variables, including the aperiodic exponent and offset.

Separate linear regression analyses were conducted to compare *ms-specparam* against both *default-specparam* and *conservative-specparam*. Chronological age and the chosen algorithm (e.g., *ms-specparam* vs. *default-specparam*) were introduced as fixed predictors, and individual participants were treated as a random factor to account for inter-individual variability.

To quantify the Bayesian evidence for each predictor in our regression models, we employed Bayes factor analysis with the Wagenmakers approximation (Wagenmakers, 2007). This provided a nuanced understanding of the statistical significance and strength of the effects of age and algorithm on spectral parameterization outcomes.

Results

Figure 1a highlights how user-dependent hyperparameters affect the outcome of spectral parameterization. In the example shown, the hyperparameter specifying the maximum number of peaks expected from spectral parameterization was set manually to a value of 6. However, the spectrum of the present empirical data contains only two peaks (left panel; Figure 1a). Under high signal-to-noise conditions, spectral parameterization may yield only two peaks as expected. However, when data is realistically noisy, the spectral parameterization algorithm may overestimate the number of peaks in the spectrum to account for noise-related fluctuations (right panel; Figure 1a). Ideally, spectral and spectrogram parameterization should automatically and adaptively adjust model hyperparameters to account for the noise level in the data.

To address these issues, we propose an approach that proceeds iteratively with the parameterization of empirical power spectra and spectrograms with increasing model complexity (i.e., the maximum number of spectral peaks). We derive the Bayesian Information Criterion (BIC) for each hyperparameter setting. The most parsimonious hyperparameter setting to model the empirical power spectrum or spectrogram is the one corresponding to the lowest BIC value (Figure 1b). If the most parsimonious model contains spectral peaks, we can further quantify the evidence for periodic activity using the Bayes factor relative to the aperiodic-only model (Figure 1c). Our approach applies to both spectral and spectrogram parameterization, as demonstrated herein with *specparam* (Donoghue et al., 2020) for spectral analysis and *SPRiNT* (Wilson et al., 2022) for spectrograms. The model-selection versions of these methods, coined *ms-specparam* and *ms-SPRiNT*, are freely available through *Brainstorm* (Tadel et al., 2011) and on GitHub (github.com/lucwilson/model_selection).

We tested and validated *ms-specparam* using 5,000 ground-truth, synthetic but neurophysiologically plausible power spectra. We compared its performance against the original *specparam* algorithm, configured to its default hyperparameters (referred to as *default-specparam*; see Methods). Additionally, we validated *ms-SPRiNT* against the original *SPRiNT* algorithm using spectrograms from 10,000 synthetic, neurophysiologically plausible time-series. We also applied *ms-specparam* to task-free MEG recordings from 606 participants to replicate, with less dependence on user-selected hyperparameters, the previously reported findings of an age-related decline in the aperiodic exponent of the neurophysiological power spectrum (Voytek et al., 2015).

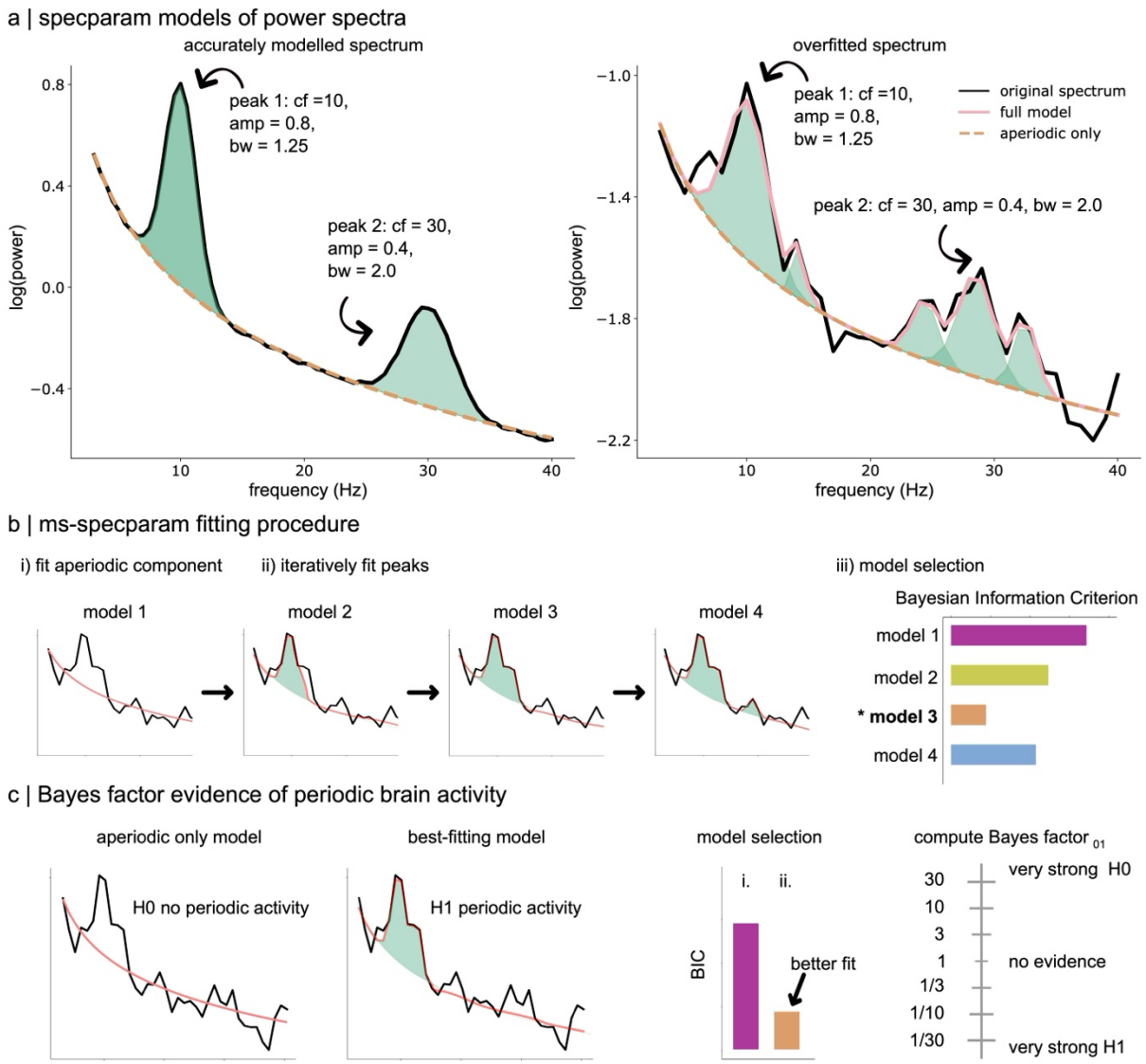

Figure 1: Spectral Parameterization with Model Selection
(a) Illustration of a spectral parameterization of a simulated power spectral density estimate (black line) obtained with *specparam* in the context of lower (left panel) and higher (right panel) noise levels. Both spectra are generated using the same spectral parameters (i.e., two spectral peaks). In more noisy conditions, *specparam* (pink line) fits a greater number of spectral peaks (green shaded areas) than what is present (simulated) in the data, resulting in overfitting (right panel). Key: '*cf*' refers to a peak's center frequency, '*amp*' refers to a peak's amplitude, and '*bw*' refers to a peak's bandwidth.
(b) *ms-specparam* is a method for spectral parameterization combined with a model selection procedure. It first adjusts a model for the aperiodic component of the spectrum (subpanel i) before adding spectral peaks (green shaded areas) in an iterative fashion (subpanel ii). These successive models are then assessed via the Bayesian Information Criterion (BIC; subpanel iii).
(c) The resulting BIC model is then subjected to Bayes factor inference against the aperiodic spectral model (panel i) to adjudicate whether spectral peaks are likely to be

present in the data power spectrum. A Bayes factor greater than 1 is evidence in favour of periodic brain activity over the null hypothesis of no periodic activity (panel iv).

Synthetic, Ground-Truth Data.

Each of the 5,000 synthetic power spectra comprised an aperiodic component, with offset values ranging from -8.1 to -1.5 arbitrary units (a.u.) and exponents set between 0.5 and 2 Hz^{-1}. We randomly added between 0 and 4 spectral peaks to the aperiodic background of each power spectrum (1,000 simulated spectra for each number of peaks; see Methods). Zero-mean Gaussian noise was added to the resulting power spectra with varying standard deviation values (s.d.).

In moderate noise conditions (s.d. = 0.10), *ms-specparam* demonstrated a slightly lower sensitivity (89%) in detecting spectral peaks compared to *default-specparam* (91%). However, it had a substantially higher positive predictive value for peak detection (*ms-specparam*: 96%; *default-specparam*: 63%). On average, *default-specparam* overestimated the number of peaks in the spectrum by 59%, whereas *ms-specparam* underestimated the number of peaks by 13% (Figure 2a). We observed similar results for sensitivity and PPV in both algorithms at lower and higher noise levels (Supplemental Materials).

We found that, on average, parameter estimates derived from *ms-specparam* are more accurate than those derived from *default-specparam*: aperiodic exponent ($t = 8.62$, $p = 0.0019$; aperiodic offset $t = 8.38$, $p = 0.0019$; peak center frequency $t = 15.33$, $p = 0.0019$; peak amplitude $t = 10.33$, $p = 0.0019$; peak bandwidth $t = 14.50$, $p = 0.0019$; one-tailed permutation t-tests; Figure 2b).

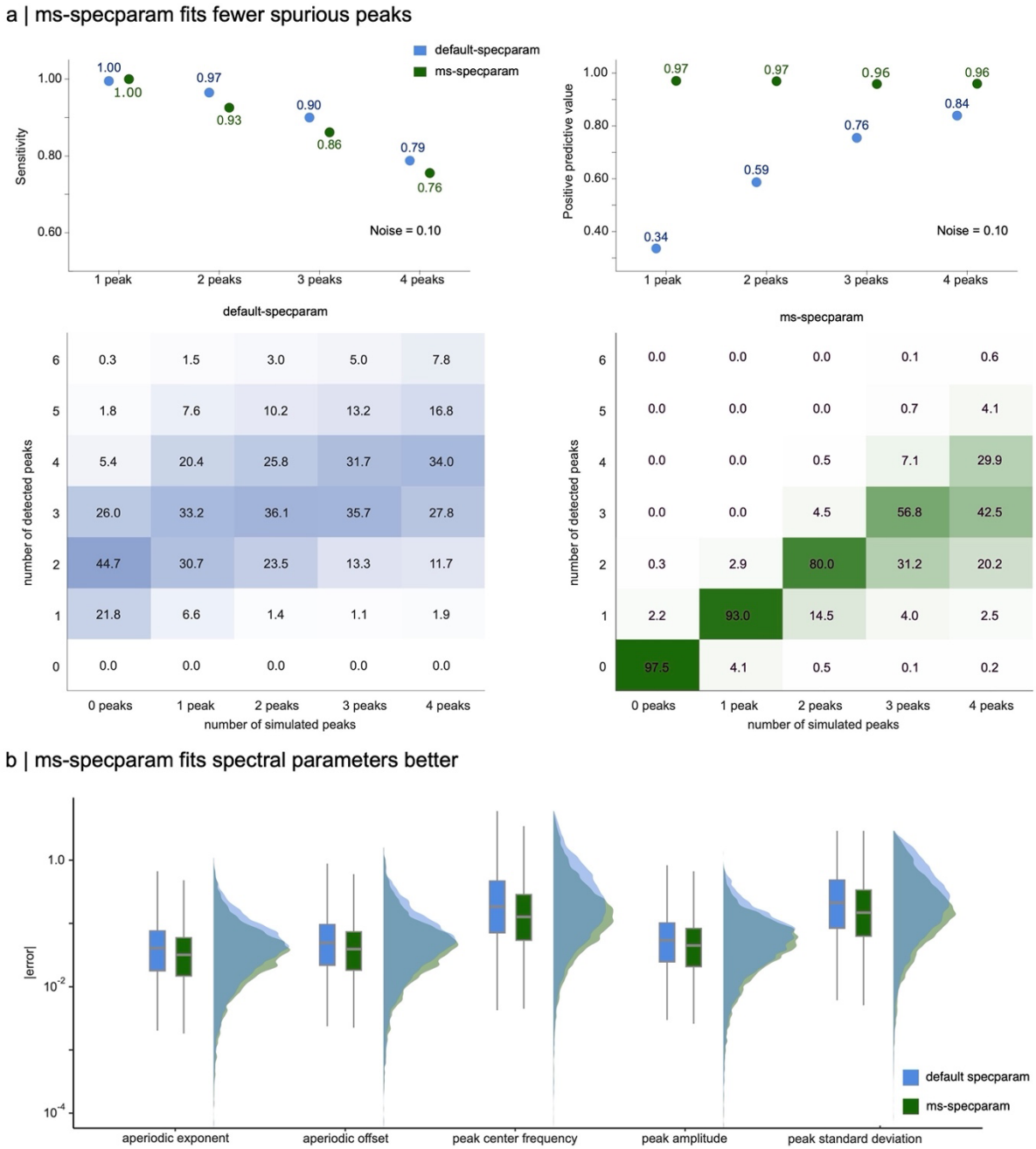

Figure 2: Performances on Synthetic Stationary Data

(a) Sensitivity and positive predictive value (PPV) for detection of spectral peaks (top row). *ms-specparam* (green) has similar sensitivity (89%) than *default-specparam* (blue; 91%), but superior PPV (96% vs. 63%). The heat maps below report the ground-truth vs. estimated number of spectral peaks (with percent incidence listed in each element) and highlight *ms-specparam*'s improved peak detection accuracy.

(b) Boxplots and empirical density distributions reporting the errors on the estimates of the spectral parameters derived using *ms-specparam* and *default-specparam*. For every

spectral parameter, *ms-specparam* estimated values with significantly lower mean absolute error (one-tailed permutation t-test, all $p<0.05$).

We subsequently evaluated the performance of *ms-SPRiNT* using 10,000 time series simulated from realistic ranges of spectral parameters. We replicated the simulation procedure of Wilson et al. (2022): in short, we synthesized neurophysiologically plausible time series (60-s duration) composed of time-varying periodic and aperiodic components (see Methods).

We evaluated the respective performances of *SPRiNT*, *SPRiNT* with post-processing (i.e., removing spurious outlier spectral peaks, following Wilson et al., 2022), *ms-SPRiNT*, and *ms-SPRiNT* with post-processing (Table S1). On average, *SPRiNT* with post-processing best estimated the number of spectral peaks (4% more than expected), than *ms-SPRiNT* (15% more than expected) and *ms-SPRiNT* with post-processing (20% fewer than expected). Similar to *specparam*, *SPRiNT* tended to overestimate the number of spectral peaks (60% more than expected; Figure 3a). *SPRiNT*'s peak detection had the highest sensitivity (89%) of all contexts (post-processing: 84%; *ms-SPRiNT*: 80%; *ms-SPRiNT* with post-processing: 76%; Figure 3b) but also the lowest positive predictive value (22%). Notably, peaks detected using *ms-SPRiNT* with post-processing had a much higher positive predictive value (83%) than all other contexts (post-processing: 45%; *ms-SPRiNT*: 43%; Figure 3d).

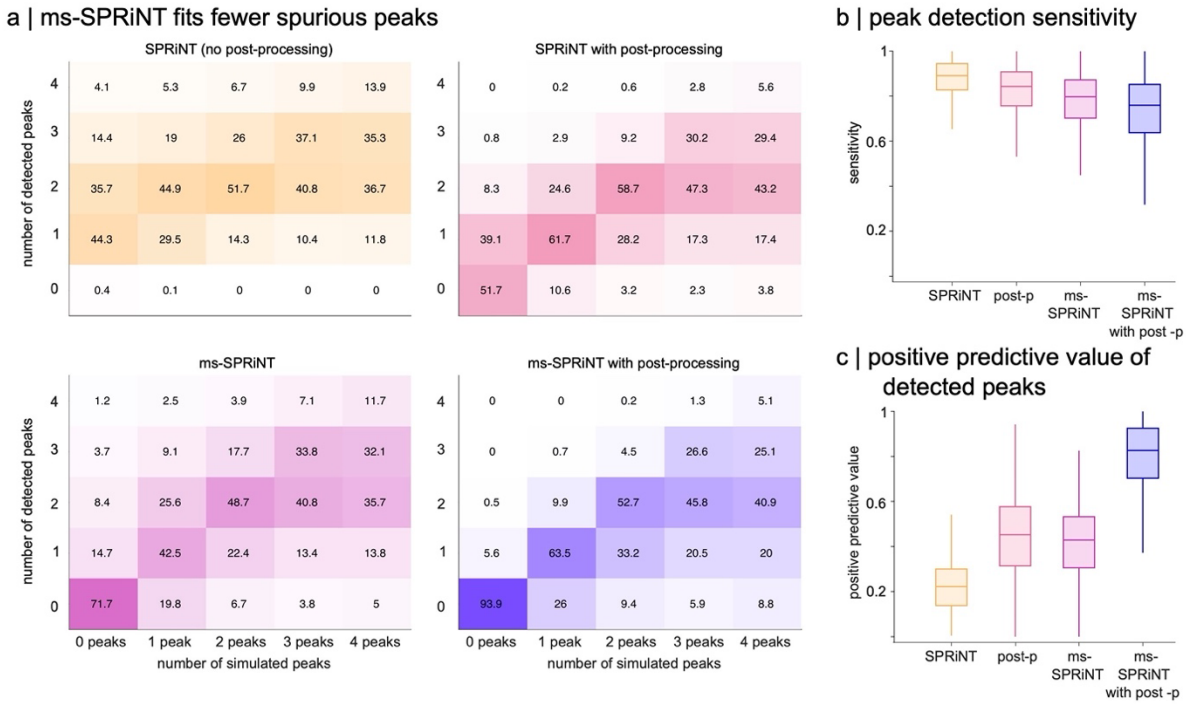

Figure 3: Performances on Synthetic Data with Time-Varying Spectral Contents
(a) Heat maps reporting the number of spectral peaks detected vs. ground-truth. *ms-SPRiNT* with post-processing (purple; bottom right) best recovers the true number of spectral peaks. Numbers of datasets synthesized with 0 spectral peaks = 798,753, 1 peak = 256,599, 2 peaks = 78,698, 3 peaks = 14,790, and 4 peaks = 1160.
(b) Sensitivity of spectral peak detection (N = 10,000 simulated time series). *ms-SPRiNT* with (purple) and without post-processing (fuchsia) exhibit marginally lower sensitivity than the default *SPRiNT* algorithm (orange).
(c) Positive predictive value (PPV) of spectral peak detection. *ms-SPRiNT* with post-processing (purple) exhibits a higher positive predictive value than all other algorithms.

Empirical MEG Data.

We applied *ms-specparam* to resting-state MEG data from the Cam-CAN repository (N=606; Shafto et al., 2014; Taylor et al., 2017). We first preprocessed and source-mapped the MEG time series using *Brainstorm* (Tadel et al., 2011) following good-practice guidelines (Gross et al., 2013). We then derived the PSDs of each cortical parcel of the Destrieux atlas (Destrieux, 2010; see Methods). We then compared models generated with *ms-specparam* to those frrom *specparam*, using two hyperparameter settings: *default-specparam* (minimum peak height: 0.1 a.u.; maximum number of peaks: 6; peak width limits: [1 8]; proximity threshold: 0.75 s.d.) and a more conservative configuration (*conservative-specparam*; minimum peak height: 0.3 a.u.; maximum number of peaks: 3; peak width limits: [0.5 12]; proximity threshold: 2).

We found that *ms-specparam* generated models with less residual variance (i.e., mean squared error, MSE; average MSE = 2.08×10^{-3}, SD = 7.68×10^{-4}) than both *specparam* settings (default:

average MSE = 3.06×10^{-3}, SD = 1.07×10^{-3}; $t = -48.82$, $p < 0.001$; conservative average MSE = 7.63×10^{-3}, SD = 3.08×10^{-3}; $t = -51.17$, $p < 0.001$; Figure 4a). This observation was consistent across all cortical parcels, with posterior parietal areas showing the greatest enhancements in model goodness-of-fit (Figure 4a). Reduced residual variance was consistent over the entire frequency range (1–40 Hz), with marked improvements with respect to both *specparam* settings over the edges of the spectrum (<5 Hz and >35 Hz; Figure 4a). We also observed that *ms-specparam* detected fewer spectral peaks than *default-specparam*, and therefore, as expected, provided more parsimonious spectral parameterizations ($t = -58.26$, $p < 0.001$; Figure 4b).

With *ms-specparam*, we performed Bayes factor analyses (Vandekerckhove et al., 2015) as an objective measure of evidence for the presence of rhythmic activity in the neurophysiological power spectrum. We found that the bilateral cuneus exhibited the highest Bayesian evidence for rhythmic activity in the resting-state, while we found the lowest evidence of rhythmic activity in the orbitofrontal and medial frontal cortices (Figure 4c).

For illustration purposes, Figure 4d shows representative spectral parameterizations obtained from neurophysiological time series recorded the right post-central gyrus. In this instance, *ms-specparam* identified two spectral peaks while *default-specparam* adjusted five spectral peaks (*default-specparam* MSE: 1.76×10^{-3}; *ms-specparam:* 1.17×10^{-3}).

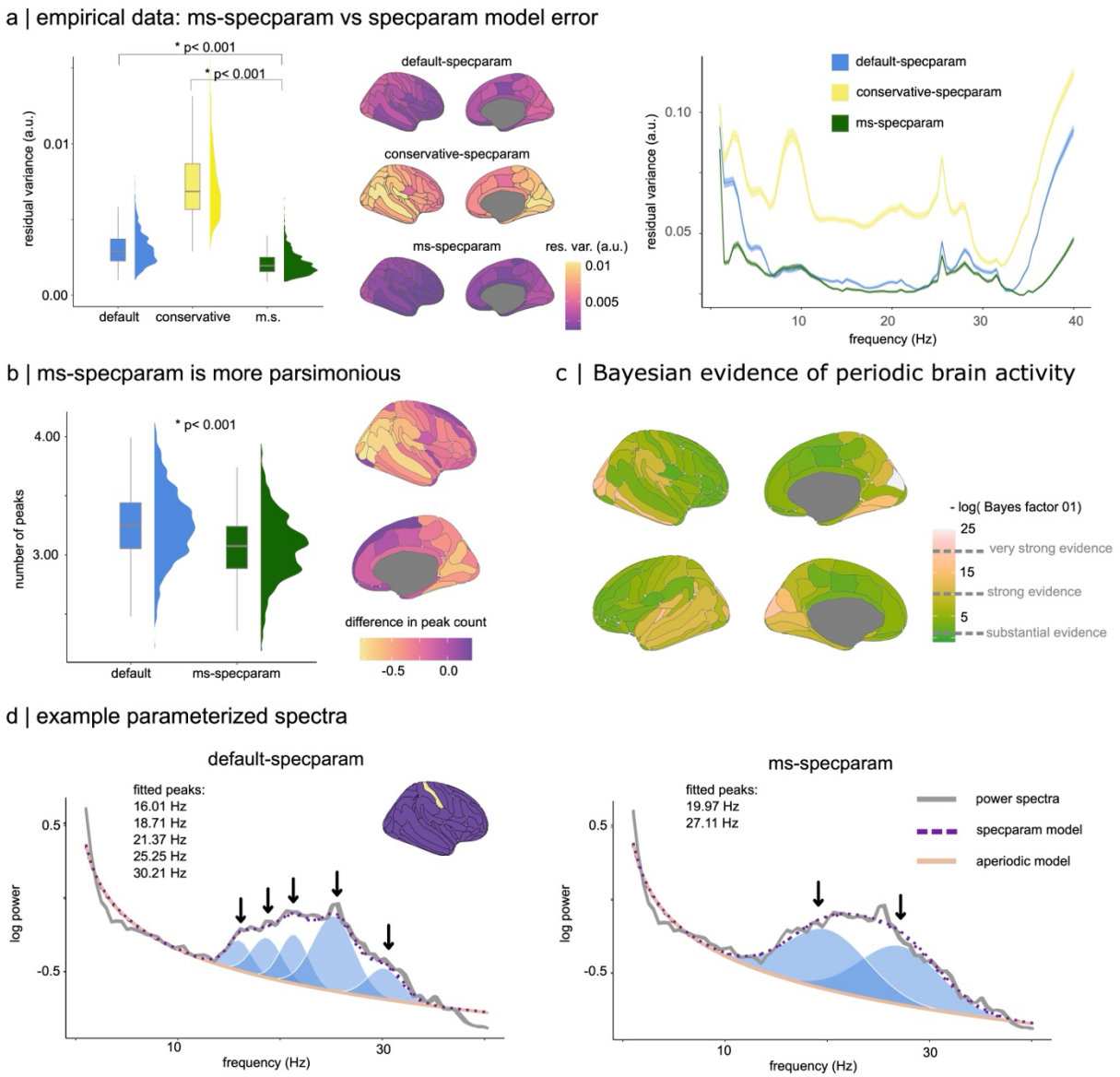

Figure 4: Performances on Empirical MEG Data.
(a) Residual variance analysis across the 606 participants and all brain regions shows *ms-specparam* (green) with consistently lower residual variance, indicating a superior fit relative to the other spectral parameterization methods (blue and yellow; left panel). The brain maps display residual variance values for each cortical parcel. A frequency breakdown (right panel) reveals *ms-specparam* outperforms the other two tested *specparam* variations across the spectrum, particularly at the edges of the frequency spectrum.
(b) *ms-specparam* estimates less spectral peaks than *default-specparam*, demonstrating more parsimonious modeling, as reported in the box/density plots (left panel). The brain maps indicate that less spectral peaks were detected in posterior cortical parcels with *ms-specparam* (right panel).
(c) Bayesian evidence for periodic, rhythmic brain activity mapped across the cortical surface emphasizes occipital and left temporal regions.

(d) Parameterized spectra from the right post-central gyrus of a sample subject highlight the differences between algorithms: *ms-specparam* fits two peaks (right panel), reflecting the dominant oscillations, whereas *default-specparam* fits five (left panel), some of which may be redundant or overfitted, as seen in the overlaid spectral models.

Age-Related Flattening of the Aperiodic Spectrum Depends on Hyperparameter Choice.

We aimed to replicate with *ms-specparam* previous observations using *specparam* of age-related decreases in aperiodic exponent (Donoghue et al., 2020; Voytek et al., 2015). We examined the degree to which the methods' hyperparameters influenced the detection of these aging effects. To do this, we fitted hierarchical linear regression models where age, the choice of spectral parameterization algorithm, and their interaction were included as predictors of both aperiodic exponent and aperiodic offset, respectively. A significant interaction would suggest that age-related changes in the spectral aperiodic exponent, for example, are contingent upon the method's hyperparameters, rather than reflecting actual neurophysiological effects.

We found that age-related decreases in aperiodic exponent are modulated by the algorithm used, whether *ms-specparam* or *specparam* with default or conservative hyperparameter settings (i.e., a significant interaction between age and spectral parameterization algorithm). This indicates that the observed age-related changes in aperiodic exponent may be influenced by the choice of parameterization method rather than solely reflecting genuine neurophysiological effects (default hyperparameters: $\beta = 0.04$, SE = 0.01, 0.02, 0.06]; $BF_{01} = 0.12$; conservative hyperparameters: $\beta = 0.12$, SE = 0.01, [0.09, 0.14]; $BF_{01} = 5.91\times10^{-12}$; Figure 5a-b and Table S2 & S3).

We obtained similar results for the age-related decline in aperiodic offset. Our analysis confirmed a significant interaction effect between age and spectral parameterization algorithm, both when comparing *ms-specparam* to *default-specparam* ($\beta = 0.04$, SE = 0.01, CI [0.01, 0.06]; $BF_{01} = 11.91$) and to *conservative-specparam* ($\beta = 0.11$, SE = 0.01, CI [0.09, 0.14]; $BF_{01} = 2.96\times10^{-13}$; Figure 5b and Table S4 & S5).

Taken together, these observations suggest that the magnitude of age-related declines in the aperiodic exponent and offset are influenced by the choice of the hyperparameters in the spectral parametrization method. Note that the effect size of age was the smallest in the spectral models derived from *ms-specparam*.

As in our simulation results, we also found that *ms-specparam* identified fewer spectral peaks than *default-specparam,* particularly in the 8-30 Hz range, and most pronounced in senior participants (65-89 years old). This reinforces the earlier finding that *ms-specparam* curtails the number of detected peaks and underscores the influence of model selection on the characterization of peak parameters across all age groups (Figure 5c).

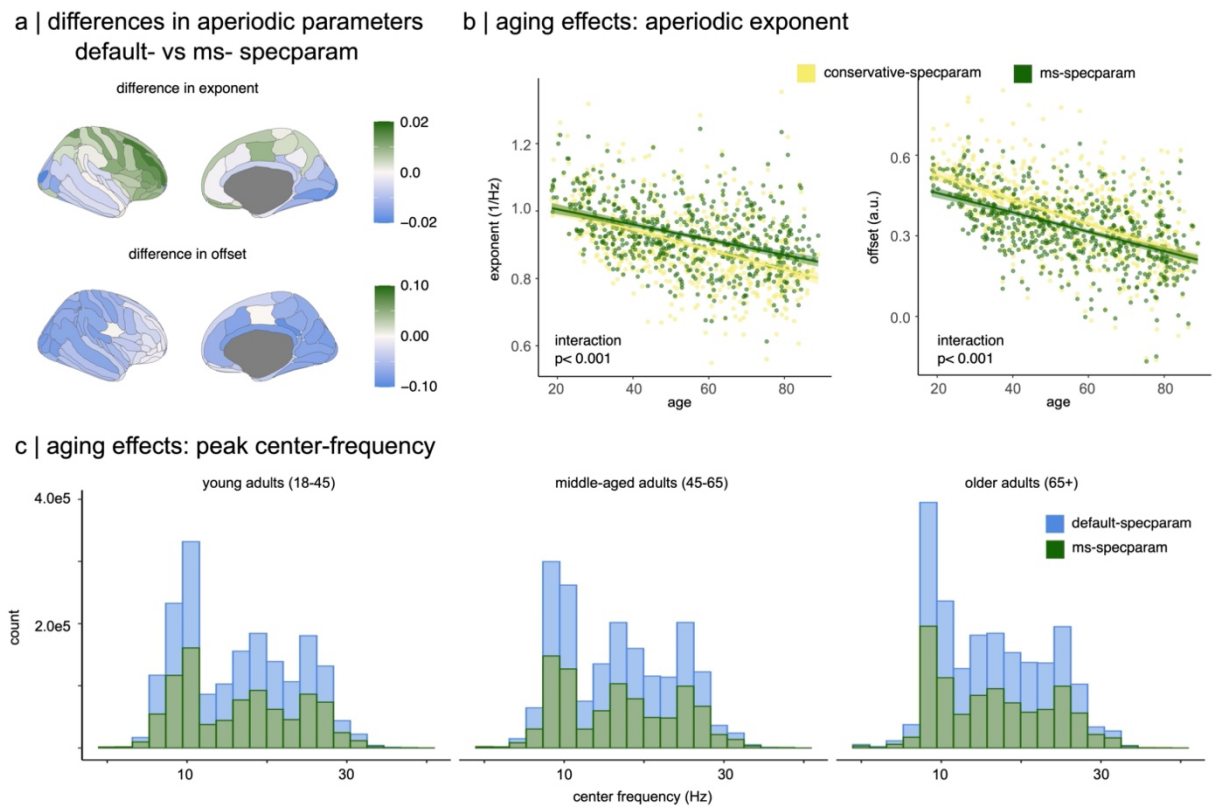

Figure 5: Age-related Neural Spectral Changes and Algorithmic Parsimony

(a) Topographical differences in aperiodic neural components, showing the variations in exponent (top) and offset (bottom) estimates when using *ms-specparam* versus *default-specparam*. Areas where *ms-specparam* yields higher parameter estimates are highlighted in blue.
(b) Moderating effect of spectral parameterization method (*ms-specparam* vs. *Default-specparam*) on the relationship between age and aperiodic spectral components. The left graph shows the exponent, and the right graph displays the offset, with statistical interactions highlighted.
(c) Frequency-specific empirical distribution of the number of peaks fitted across different age groups. The histograms show that *ms-specparam* (green) generally fits fewer peaks, especially in the mid-frequency range (8-30Hz), illustrating a more parsimonious approach to model fitting and potentially more accurate reflection of age-related spectral changes.

Discussion

Spectral parameterization enables the spectral decomposition of neurophysiological signals into aperiodic and periodic components. Its adoption has grown rapidly over recent years, thanks to open software tools, with the aim of disambiguating the respective functions of rhythmic oscillatory and arrhythmic background neural activity. However, present tools require the manual adjustment of algorithm parameters (hyperparameters), which hinders the reproducibility, interpretability, and proper fitting of spectral parameterization models to the empirical data. In the present report, we addressed this issue with the addition of a principled model selection strategy to *specparam* (*ms-specparam*) and *SPRiNT* (*ms-SPRiNT*) to set key hyperparameters, including the maximum number of peaks, minimum peak height, and proximity threshold. We validated both new methods with synthetic and empirical data. We show that the resulting spectral parameterizations are more parsimonious and fit better the data, while being considerably less dependent on user decisions and expertise.

Spectral Parameterization with Enhanced Model Parsimony and Goodness-of-Fit.

Our examination of ground-truth data shows that *ms-specparam* is more effective that *specparam* in accurately identifying spectral peaks. It avoids the frequent issue in practice of overfitting the spectral data, which typically overestimates the number of periodic components in power spectra (Figure 2a). In empirical data also, *ms-specparam* consistently generates more parsimonious models (Figure 4). We observed enhanced goodness-of-fit (reduced residual variance) in both synthetic and real-world data (Figures 2b and 4a), particularly at the edges of the frequency spectrum. The implications of these findings are twofold: firstly, *ms-specparam*'s parsimonious approach prevents both overfitting and *underfitting* (see Practical Guidelines below). Secondly, the improved accuracy of aperiodic component estimates is critical for characterizing complex neural dynamics (Donoghue et al., 2020; Gerster et al., 2022).

The proposed model selection approach features similar benefits for the parameterization of spectrograms, with substantial improvements of the model's positive predictive values and less parameter settings than the ad-hoc post-processing steps proposed by Wilson et al. (2022). We note, however, that combining model selection with post-processing increases dramatically the positive predictive value of detected peaks (83% vs. about 45% for model-selection only), with only a modest reduction (approximately 8%) in peak sensitivity.

To understand why the benefits of post-processing and model selection are additive, we can consider the mechanism by which they achieve more parsimonious fits. Post-processing removes isolated spectral peaks in time and frequency. Model selection encourages the parsimonious addition of spectral peaks to the model, observing both goodness-of-fit and BIC. When combined, model selection and post-processing remove spectral peaks which either do not substantially improve goodness-of-fit (model selection) or have short durations (post-processing).

Hyperparameter Settings.

Our empirical investigations emphasize the critical role of hyperparameter settings in spectral modelling. Notably, the choice of spectral parameterization algorithm influenced aperiodic parameter estimates across methods (Figures 5a-c). While deviations were modest, suggesting that default spectral parameterizations may have captured the aperiodic component accurately, our comparative analysis with synthetic data indicates that *ms-specparam* yields improved estimates of the aperiodic exponent and offset (Figure 2b).

We replicated with the new model selection approach previous observations of changing aperiodic parameters with age (Cellier et al., 2021; Donoghue et al., 2020; Hill et al., 2022). We found that the aperiodic component of the neurophysiological power spectrum flattens with age, which has been discussed as related to increased neural noise and asynchronous neuronal firing, yielding less structured brain dynamics (Usher et al., 1995; Pozzorini et al., 2013; Voytek et al., 2015; Voytek & Knight, 2015). Several empirical observations support this hypothesis (Hanggi and Jung, 1994; Bédard et al., 2006; Sosnoff and Newell, 2011).

We found, however, that previously reported effects of shifts in the spectral aperiodic exponent and offset with age can be substantially reduced, depending on the spectral parameterization method used and its hyperparameters. This observation encourages the present and further efforts towards more automated and principled parameter selection procedures, promoting robustness and replicability of research results.

Practical Guidelines.

We provide practical recommendations to adjust the hyperparameters of *ms-specparam*. As with other spectral parameterization methods, we encourage future users to examine their data's power spectra before and after applying *ms-specparam* and verify the model's goodness-of-fit. We refer the reader to the previously published guidelines by Donoghue et al. (2020), Gerster et al. (2022), and Ostlund et al. (2022), which set good foundational principles for neurophysiological spectral parameterization. Here, we highlight more specific considerations for the best possible use of *ms-specparam*:

1. Model selection in *ms-specparam* determines the optimal number of spectral peaks that fit the empirical power spectrum. The setting of other hyperparameters, including peak width limits and aperiodic mode, remain to be defined by the user. The value set for the maximum number of spectral peaks parameter needs to be larger than the number of peaks that are clearly visible in the data's power spectrum. In our investigations, we set this value to 6.
2. We encourage users to derive measures of model goodness-of-fit, such as Mean-Squared Error, R^2, and BIC, as in our *Brainstorm* plug-in of the proposed model selection methods. Some of these metrics, like R^2, may be influenced by the aperiodic component of the spectrum, as demonstrated in previous studies (Donoghue et al., 2020). In the context of model selection, users should choose the spectral model with the lowest BIC (as in the present study).

These guidelines also apply to time-resolved spectral parameterization with *ms-SPRiNT*. Model selection enhances the positive predictive value of detected spectral peaks and may substitute for

post-processing (Wilson et al., 2022). Post-processing requires users to set additional hyperparameters.

To conclude, the present report introduced a model selection approach to the parameterization of neurophysiological power spectra and spectrograms. The approach minimizes the requirement for user expertise in the adjustment of hyperparameters, which influences the outcome of analyses. It is grounded in the optimization of parameters that favour model parsimony while maximizing goodness-of-fit. We foresee that this principled approach will contribute to the robust application of spectral parameterization in neuroscience research, further elucidating the roles of rhythmic and arrhythmic brain activity in cognition, health, and disease. We anticipate that the proposed tools, *ms-specparam* and *ms-SPRiNT*, will enhance the reproducibility and robustness of reported findings.

Data and Software Availability

The *ms-specparam* and *ms-SPRiNT* algorithms, as well as simulated power spectra and code used to generate results, are available on GitHub (github.com/lucwilson/model_selection). Simulated neural-like time series used for spectrogram parameterization can be accessed from Wilson et al. (2022). Resting-state MEG recordings were obtained from the CamCAN repository (Shafto et al., 2014; Taylor et al., 2017).

Author Contributions

Conceptualization: LEW, JDSC
Data Curation: LEW, JDSC
Methodology: LEW, JDSC, BLK
Software: LEW, JDSC
Visualization: LEW, JDSC, BLK
Funding acquisition: SB
Writing – original draft: LEW, JDSC, SB
Writing – review & editing: LEW, JDSC, BLK, SB

Declaration of Competing Interests

All authors declare no competing conflicts of interest. The listed funding sources in the **Acknowledgements** did not play any role in the writing of the manuscript or the decision to submit this manuscript for publication.

Acknowledgements

The Brainstorm app is supported by funding to SB from the NIH (R01-EB026299), a Discovery grant from the Natural Science and Engineering Research Council of Canada (436355-13), the CIHR Canada Research Chair in Neural Dynamics of Brain Systems, the Brain Canada Foundation with support from Health Canada, and the Innovative Ideas program from the Canada First Research Excellence Fund, awarded to McGill University for the HBHL initiative. This work was

supported by a doctoral fellowship from NSERC (JDSC), as well as by a master's fellowship from NSERC (LEW).

Supplemental Materials

Algorithm Validation with Alternative Noise Conditions.

In addition to injecting moderate noise to the synthetic data, we also evaluated *ms-specparam* performance at low (s.d. = 0.05) and high (s.d. = 0.15) noise conditions. In spectra with low noise, *ms-specparam* detected spectral peaks with comparable sensitivity (92%) to *default-specparam* (92%). The positive predictive value of peaks detected using *ms-specparam* (97%) was notably higher than that of peaks detected using *default-specparam* (68%). In spectra with high noise, *ms-specparam* detected spectral peaks with lower sensitivity (84%) to *default-specparam* (90%). However, the positive predictive value of peaks detected using *ms-specparam* (96%) remained higher than that of peaks detected using *default-specparam* (61%). Taken together, these results support the generalizability of the observed algorithmic performance improvements across noise levels.

	exponent		**offset**		**cent. freq.**		**amplitude**		**st. dev.**	
Parameter estimation error	*Mean*	*SE*	*Mean*	*SE*	*Mean*	*SE*	*Mean*	*SE*	*Mean*	*SE*
SPRiNT	0.16	$5x10^{-4}$	0.21	$5x10^{-4}$	0.59	$9x10^{-4}$	0.24	$8x10^{-4}$	0.24	$5x10^{-4}$
SPRiNT with post-processing	0.13	$5x10^{-4}$	0.16	$5x10^{-4}$	0.49	$9x10^{-4}$	0.24	$8x10^{-4}$	0.24	$5x10^{-4}$
ms-SPRiNT	0.15	$5x10^{-4}$	0.19	$5x10^{-4}$	0.49	$9x10^{-4}$	0.24	$8x10^{-4}$	0.24	$5x10^{-4}$
ms-SPRiNT with post-processing	0.12	$5x10^{-4}$	0.15	$5x10^{-4}$	0.41	$9x10^{-4}$	0.23	$9x10^{-4}$	0.23	$5x10^{-4}$

Table S1. Parameter estimation error for spectrograms with and without model selection.

		exponent	
Predictors	*Estimates*	*CI*	*p*
(Intercept)	0.00	-0.07 – 0.08	0.944
algorithm [default vs ms-specparam]	-0.01	-0.03 – 0.01	0.610
age (continuous)	-0.44	-0.51 – -0.37	**<0.001**
algorithm [default vs ms-specparam] × age (continuous)	0.04	0.02 – 0.06	**<0.001**
Random Effects			
σ^2	0.03		
$\tau_{00\ subID}$	0.80		
ICC	0.96		
N_{subID}	606		
Observations	1212		
Marginal R^2 / Conditional R^2	0.174 / 0.969		

Table S2. Hyperparameter choice impacts the age's effect on the aperiodic exponent: default hyperparameter setting vs *ms-specparam*.

	exponent		
Predictors	*Estimates*	*CI*	*p*
(Intercept)	-0.12	-0.19 – -0.05	**0.001**
algorithm [conservative vs ms-specparam]	0.24	0.21 – 0.26	**<0.001**
age (continuous)	-0.50	-0.57 – -0.43	**<0.001**
algorithm [conservative vs ms-specparam] × age (continuous)	0.12	0.09 – 0.14	**<0.001**
Random Effects			
σ^2	0.06		
$\tau_{00\ subID}$	0.73		
ICC	0.93		
N_{subID}	606		
Observations	1212		
Marginal R^2 / Conditional R^2	0.209 / 0.942		

Table S3. Hyperparameter choice impacts the age's effect on the aperiodic exponent: conservative hyperparameter setting vs *ms-specparam*.

	offset		
Predictors	*Estimates*	*CI*	*p*
(Intercept)	0.19	0.13 – 0.26	**<0.001**
algorithm [default vs ms-specparam]	-0.39	-0.41 – -0.36	**<0.001**
age raw	-0.52	-0.59 – -0.46	**<0.001**
algorithm [default vs ms-specparam] × age raw	0.04	0.01 – 0.06	**0.002**
Random Effects			
σ^2	0.04		
$\tau_{00\ subID}$	0.67		
ICC	0.94		
N_{subID}	606		
Observations	1212		
Marginal R^2 / Conditional R^2	0.294 / 0.960		

Table S4. Hyperparameter choice impacts the age's effect on the aperiodic offset: default hyperparameter setting vs *ms-specparam*.

	offset		
Predictors	*Estimates*	*CI*	*p*
(Intercept)	0.12	0.05 – 0.19	**<0.001**
algorithm [conservative vs ms-specparam]	-0.24	-0.27 – -0.22	**<0.001**
age raw	-0.58	-0.65 – -0.52	**<0.001**
algorithm [conservative vs ms-specparam] × age raw	0.11	0.09 – 0.14	**<0.001**
Random Effects			
σ^2	0.05		
$\tau_{00\ subID}$	0.66		
ICC	0.93		
N_{subID}	606		
Observations	1212		
Marginal R^2 / Conditional R^2	0.294 / 0.948		

Table S5. Hyperparameter choice impacts the age's effect on the aperiodic offset: conservative hyperparameter setting vs *ms-specparam*.

References

Bédard, C., Kröger, H., & Destexhe, A. (2006). Does the 1/f frequency scaling of brain signals reflect self-organized critical states? *Physical Review Letters, 97*(11), 118102. doi:10.1103/PhysRevLett.97.118102

Brady, B., & Bardouille, T. (2022). Periodic/aperiodic parameterization of transient oscillations (PAPTO)-Implications for healthy ageing. *NeuroImage, 251*, 118974. doi:10.1016/j.neuroimage.2022.118974

Brake, N., Duc, F., Rokos, A., Arseneau, F., Shahiri, S., Khadra, A., & Plourde, G. (2024). A neurophysiological basis for aperiodic EEG and the background spectral trend. *Nature Communications, 15*(1), 1514. doi:10.1038/s41467-024-45922-8

Buzsáki, G., & Watson, B. O. (2012). Brain rhythms and neural syntax: Implications for efficient coding of cognitive content and neuropsychiatric disease. *Dialogues in Clinical Neuroscience, 14*(4), 345-367. doi:10.31887/DCNS.2012.14.4/gbuzsaki

Cellier, D., Riddle, J., Petersen, I., & Hwang, K. (2021). The development of theta and alpha neural oscillations from ages 3 to 24 years. *Developmental Cognitive Neuroscience, 50*, 100969. doi:10.1016/j.dcn.2021.100969

Chini, M., Pfeffer, T., & Hanganu-Opatz, I. (2022). An increase of inhibition drives the developmental decorrelation of neural activity. *eLife, 11*, e78811. doi:10.7554/eLife.78811

Cole, S., Donoghue, T., Gao, R., & Voytek, B. (2019). NeuroDSP: A package for neural digital signal processing. *Journal of Open Science Software, 4*(36). doi:10.21105/joss.01272

da Silva Castanheira, J., Orozco Perez, H. D., Misic, B., & Baillet, S. (2021). Brief segments of neurophysiological activity enable individual differentiation. *Nature Communications, 12*(1), 5713. doi:10.1038/s41467-021-25895-8

Destrieux, C., Fischl, B., Dale, A., & Halgren, E. (2010). Automatic parcellation of human cortical gyri and sulci using standard anatomical nomenclature. *NeuroImage, 53*(1), 1-15. doi:10.1016/j.neuroimage.2010.06.010

Donoghue, T., Haller, M., Peterson, E. J., Varma, P., Sebastian, P., Gao, R., . . . Voytek, B. (2020). Parameterizing neural power spectra into periodic and aperiodic components. *Nature Neuroscience, 23*(12), 1655-1665. doi:10.1038/s41593-020-00744-x

Fischl, B. (2012). FreeSurfer. *NeuroImage, 62*(2), 774-781. doi:10.1016/j.neuroimage.2012.01.021

Gao, R., Peterson, E. J., & Voytek, B. (2017). Inferring synaptic excitation/inhibition balance from field potentials. *NeuroImage, 158*, 70-78. doi:10.1016/j.neuroimage.2017.06.078

Gerster, M., Waterstraat, G., Litvak, V., Lehnertz, K., Schnitzler, A., Florin, E., . . . Nikulin, V. (2022). Separating neural oscillations from aperiodic 1/f activity: Challenges and recommendations. *Neuroinformatics*. doi:10.1007/s12021-022-09581-8

Gross, J., Baillet, S., Barnes, G. R., Henson, R. N., Hillebrand, A., Jensen, O., . . . Schoffelen, J.-M. (2013). Good practice for conducting and reporting MEG research. *NeuroImage, 65*, 349-363. doi:10.1016/j.neuroimage.2012.10.001

Gyurkovics, M., Clements, G. M., Low, K. A., Fabiani, M., & Gratton, G. (2022). Stimulus-induced changes in 1/f-like background activity in EEG. *The Journal of Neuroscience, 42*(37), 7144. doi:10.1523/JNEUROSCI.0414-22.2022

Häunggi, P., & Jung, P. (1994). Colored noise in dynamical systems. In *Advances in Chemical Physics* (pp. 239-326).

Hill, A. T., Clark, G. M., Bigelow, F. J., Lum, J. A. G., & Enticott, P. G. (2022). Periodic and aperiodic neural activity displays age-dependent changes across early-to-middle childhood. *Developmental Cognitive Neuroscience, 54*, 101076. doi:https://doi.org/10.1016/j.dcn.2022.101076

Jefferys, W. H., & Berger, J. O. (1992). Ockham's Razor and Bayesian Analysis. *American Scientist, 80*(1), 64-72. Retrieved from http://www.jstor.org/stable/29774559.

Kosciessa, J. Q., Grandy, T. H., Garrett, D. D., & Werkle-Bergner, M. (2020). Single-trial characterization of neural rhythms: Potential and challenges. *NeuroImage, 206*, 116331. doi:10.1016/j.neuroimage.2019.116331

Miller, K. J., Honey, C. J., Hermes, D., Rao, R. P. N., denNijs, M., & Ojemann, J. G. (2014). Broadband changes in the cortical surface potential track activation of functionally diverse neuronal populations. *NeuroImage, 85*, 711-720. doi:10.1016/j.neuroimage.2013.08.070

Mitchell, T. M. (1997). *Machine Learning*. New York: McGraw-Hill.

Myung, I. J. (2000). The importance of complexity in model selection. *Journal of Mathematical Psychology, 44*(1), 190-204. doi:10.1006/jmps.1999.1283

Ostlund, B., Donoghue, T., Anaya, B., Gunther, K. E., Karalunas, S. L., Voytek, B., & Pérez-Edgar, K. E. (2022). Spectral parameterization for studying neurodevelopment: How and why. *Developmental Cognitive Neuroscience, 54*, 101073. doi:10.1016/j.dcn.2022.101073

Ostlund, B. D., Alperin, B. R., Drew, T., & Karalunas, S. L. (2021). Behavioral and cognitive correlates of the aperiodic (1/f-like) exponent of the EEG power spectrum in adolescents with and without ADHD. *Developmental Cognitive Neuroscience, 48*, 100931. doi:10.1016/j.dcn.2021.100931

Pozzorini, C., Naud, R., Mensi, S., & Gerstner, W. (2013). Temporal whitening by power-law adaptation in neocortical neurons. *Nature Neuroscience, 16*(7), 942-948. doi:10.1038/nn.3431

Preston, M., Schaworonkow, N., & Voytek, B. (2022). Oscillations and aperiodic activity: Evidence for dynamic changes in both during memory encoding. *bioRxiv*, 2022.2010.2004.509632. doi:10.1101/2022.10.04.509632

Schwarz, G. (1978). Estimating the dimension of a model. *The Annals of Statistics, 6*(2), 461-464. doi:10.1214/aos/1176344136

Seymour, R. A., Alexander, N., & Maguire, E. A. (2022). Robust estimation of 1/f activity improves oscillatory burst detection. *European Journal of Neuroscience, 56*(10), 5836-5852. doi:10.1111/ejn.15829

Shafto, M. A., Tyler, L. K., Dixon, M., Taylor, J. R., Rowe, J. B., Cusack, R., . . . Cam-CAN (2014). The Cambridge Centre for Ageing and Neuroscience (Cam-CAN) study protocol: A cross-sectional, lifespan, multidisciplinary examination of healthy cognitive ageing. *BMC Neurology, 14*(1), 204. doi:10.1186/s12883-014-0204-1

Sosnoff, J. J., & Newell, K. M. (2011). Aging and motor variability: A test of the neural noise hypothesis. *Experimental Aging Research, 37*(4), 377-397. doi:10.1080/0361073X.2011.590754

Stokes, P. A., Rath, P., Possidente, T., He, M., Purcell, S., Manoach, D. S., . . . Prerau, M. J. (2023). Transient oscillation dynamics during sleep provide a robust basis for electroencephalographic phenotyping and biomarker identification. *Sleep, 46*(1), zsac223. doi:10.1093/sleep/zsac223

Tadel, F., Baillet, S., Mosher, J. C., Pantazis, D., & Leahy, R. M. (2011). Brainstorm: A user-friendly application for MEG/EEG analysis. *Computational Intelligence and Neuroscience, 2011*, 879716. doi:10.1155/2011/879716

Taylor, J. R., Williams, N., Cusack, R., Auer, T., Shafto, M. A., Dixon, M., . . . Henson, R. N. (2017). The Cambridge Centre for Ageing and Neuroscience (Cam-CAN) data repository: Structural and functional MRI, MEG, and cognitive data from a cross-sectional adult lifespan sample. *NeuroImage, 144*, 262-269. doi:10.1016/j.neuroimage.2015.09.018

Usher, M., Stemmler, M., & Olami, Z. (1995). Dynamic pattern formation leads to 1/f noise in neural populations. *Physical Review Letters, 74*(2), 326-329. doi:10.1103/PhysRevLett.74.326

Vandekerckhove, J., Matzke, D., & Wagenmakers, E.-J. (2015). Model comparison and the principle of parsimony. In *The Oxford Handbook of Computational and Mathematical Psychology.* doi:10.1093/oxfordhb/9780199957996.013.14

Voytek, B., & Knight, R. T. (2015). Dynamic network communication as a unifying neural basis for cognition, development, aging, and disease. *Biological Psychiatry, 77*(12), 1089-1097. doi:10.1016/j.biopsych.2015.04.016

Voytek, B., Kramer, M. A., Case, J., Lepage, K. Q., Tempesta, Z. R., Knight, R. T., & Gazzaley, A. (2015). Age-related changes in 1/f neural electrophysiological noise. *The Journal of Neuroscience, 35*(38), 13257. doi:10.1523/JNEUROSCI.2332-14.2015

Wagenmakers, E.-J. (2007). A practical solution to the pervasive problems of p values. *Psychonomic Bulletin & Review, 14*(5), 779-804. doi:10.3758/BF03194105

Waschke, L., Donoghue, T., Fiedler, L., Smith, S., Garrett, D. D., Voytek, B., & Obleser, J. (2021). Modality-specific tracking of attention and sensory statistics in the human electrophysiological spectral exponent. *eLife, 10*, e70068. doi:10.7554/eLife.70068

Wen, H., & Liu, Z. (2016). Separating fractal and oscillatory components in the power spectrum of neurophysiological signal. *Brain Topography, 29*(1), 13-26.

Whitten, T. A., Hughes, A. M., Dickson, C. T., & Caplan, J. B. (2011). A better oscillation detection method robustly extracts EEG rhythms across brain state changes: The human alpha rhythm as a test case. *NeuroImage, 54*(2), 860-874. doi:10.1016/j.neuroimage.2010.08.064

Wiesman, A. I., da Silva Castanheira, J., & Baillet, S. (2022). Stability of spectral estimates in resting-state magnetoencephalography: Recommendations for minimal data duration with neuroanatomical specificity. *NeuroImage, 247*, 118823. doi:10.1016/j.neuroimage.2021.118823

Wiest, C., Torrecillos, F., Pogosyan, A., Bange, M., Muthuraman, M., Groppa, S., . . . Tan, H. (2023). The aperiodic exponent of subthalamic field potentials reflects excitation/inhibition balance in Parkinsonism. *eLife, 12*, e82467. doi:10.7554/eLife.82467

Wilson, L. E., da Silva Castanheira, J., & Baillet, S. (2022). Time-resolved parameterization of aperiodic and periodic brain activity. *eLife, 11*, e77348. doi:10.7554/eLife.77348